

ORNL/TM-2000/362

**Study of the Potential Impact of Gamma-Induced Radiolytic Gases
on Loading of Cesium Onto Crystalline Silicotitanate
Sorbent at ORNL's High Flux Isotope Reactor**

A. J. Mattus
T. E. Kent
P. A. Taylor

Chemical Technology Division

**Study of the Potential Impact of Gamma-Induced Radiolytic Gases
on Loading of Cesium Onto Crystalline Silicotitanate
Sorbent at ORNL's High Flux Isotope Reactor**

A. J. Mattus
T. E. Kent
P. A. Taylor

January 2001

Prepared by the
OAK RIDGE NATIONAL LABORATORY
Oak Ridge, Tennessee 37831-6285
managed by
UT-BATTELLE, LLC
for the
U.S. DEPARTMENT OF ENERGY
under contract DE-AC05-00OR22725

CONTENTS

LIST OF FIGURES	v
LIST OF TABLES	v
EXECUTIVE SUMMARY	vii
1. INTRODUCTION	1
2. DESCRIPTION OF THE HFIR FACILITY	3
3. EXPERIMENTAL SETUP AND OPERATION	4
3.1 EQUIPMENT	6
3.1.1 CST Column	6
3.1.2 CST Column and Can Assembly	8
3.1.3 Column and Spent-Fuel-Element Arrangement	8
3.1.4 In-Pool Experimental Setup	12
3.1.5 Skid Configuration and Operation	13
3.2 DEVIATIONS FROM THE ORIGINAL TECHNICAL TASK PLAN	17
4. MATERIALS AND METHODS	18
4.1 SIMULANT SATURATION PARAMETERS	19
4.2 PRELIMINARY PUMPING TESTS	21
5. ANALYTICAL METHODS	22
5.1 SIMULANT FEED AND COLUMN EFFLUENT	22
5.2 RADIOLYTICALLY FORMED GASES	24
6. RESULTS	24
6.1 RADIOLYTIC GASES	24
6.2 CESIUM BREAKTHROUGH CURVES	26
6.3 CST X-RAY SPECTRA	28
7. CONCLUSIONS	28
8. ACKNOWLEDGMENTS	30
9. REFERENCES	30

LIST OF FIGURES

<u>Figure</u>		<u>Page</u>
1	CST column with attached simulant and cooling lines	7
2	CST column secured inside the standard outer can	9
3	Cutaway view of the column and can assembly	10
4	Cross-sectional view of the column and can inside the spent fuel element	11
5	In-pool experimental setup, showing the attached umbilical hose	12
6	Schematic of the experimental equipment layout at the HFIR pool	14
7	Cesium fractional breakthrough curves	27
8	X-ray spectra of irradiated and unirradiated CST	29

LIST OF TABLES

<u>Table</u>		<u>Page</u>
1	Composition of high-nitrate simulant used in CST tests	23
2	Gas analyses by mass spectrometry	26

EXECUTIVE SUMMARY

The use of an engineered form of crystalline silicotitanate as a potential sorbent for the removal and concentration of cesium from the high-level waste at the Savannah River Site was investigated. Results conclusively showed this sorbent to be unaffected by gamma-induced radiolytic gas formation during column loading. Closely controlled column-loading experiments were performed at the Oak Ridge National Laboratory's High Flux Isotope Reactor (HFIR) in a gamma field with a conservative dose rate expected to exceed that in a full-scale column by a factor of nearly 16. Operation of column loading under expected nominal full-scale field conditions in the HFIR pool showed that radiolytic gases were formed at a previously calculated generation rate of 0.4 mL per liter of feed solution. When the resulting cesium-loading curve in the gamma field was compared with that of a control experiment in the absence of a gamma field, no discernable difference in the curves (within analytical error) was detected. Both curves were in good agreement with the VERSE computer-generated curve. Results conclusively indicate that the production of radiolytic gases within a full-scale column is not expected to result in reduced capacity or associated gas generation problems during operation at the Savannah River Site.

1. INTRODUCTION

Through the Salt Processing Project (SPP), the Department of Energy (DOE) has tasked the Savannah River Site (SRS) with the treatment and disposition of the high-level waste (HLW) stored on-site. The overall SPP encompasses the selection, design, construction, and operation of facilities to treat the soluble HLW.¹ Following treatment, the decontaminated liquid would go to the site's Saltstone Facility, and the sludge would go to a borosilicate-based vitrification facility known as the Defense Waste Processing Facility (DWPF).¹ Radioactive elements such as the actinides, strontium, and cesium will be removed from the liquids and will become feed to the DWPF vitrifier.

The In-Tank Precipitation (ITP) process using tetraphenylborate (TPB) to precipitate cesium was studied extensively during the 1980s at SRS and tested in 1995 with radioactive waste. Problems with the coproduction of large amounts of the degradation product benzene caused some safety concerns. Eventually, in August 1996, the Defense Nuclear Facilities Safety Board (DNFSB) advised (Recommendation 96-1) that operations and testing in the ITP Facility not proceed until the mechanism(s) involved in TPB degradation are more fully understood. As a result of the benzene problem with the ITP process, other alternatives for removing cesium from HLW were evaluated.

An engineering evaluation of more than 140 potential cesium-removal processes eventually produced a final list of four candidates. These choices were the use of a nonelutable silicotitanate sorbent, a caustic side solvent extraction, a small-tank TPB precipitation, and cement-based grouting with no cesium removal; further review eliminated the direct grouting option. The National Academy of Sciences is independently overseeing the DOE evaluation of the technologies with the support of the Tanks Focus Area (TFA). This study is a part of the comprehensive R&D program plan for the technology evaluation that the TFA is to prepare and manage. A DOE decision as to which technology will move forward at SRS is expected by June 2001.¹

In the currently proposed nonelutable ion-exchange process utilizing crystalline silicotitanate (CST), soluble alpha contaminants and ⁹⁰Sr would first be sorbed onto monosodium titanate in an alpha sorption tank and then washed and filtered, yielding a solution of approximately 5.6 M sodium. An acceptable filtrate from this process step would become the feed to an ion-exchange-column train charged with an engineered form of CST.

As described in the TFA Project R&D Program plan,¹ the ion-exchange train would be made up of three columns in series, employing downflow feed with a fourth column in standby for use during column change out. When the first is fully loaded (~90% capacity), it will be removed from service and the standby column will be used as the third of the primary columns. The CST in the first loaded column will be sluiced with water to a holding tank. Following a solid-liquid separation step, the CST will be transferred to the DWPF for incorporation into HLW glass.

The preliminary design specifies 20-ft-tall fixed columns that are 5 ft in diameter with a 16-ft-high bed. Each can load up to 5 MCi of ¹³⁷Cs. Consequently, radiolytic gas generation from gamma radiolysis of water and nitrate is expected to yield oxygen, hydrogen, and, possibly, lower oxides of nitrogen, although these oxides were not observed in the work reported here. It has been estimated that as much as 35 L/h of gas will be produced within a loaded column from ~5 MCi of ¹³⁷Cs.¹ Walker has shown that oxygen is the major gas formed from the high-nitrate waste, while in the high-hydroxide waste, hydrogen is formed in larger amounts than oxygen. High-nitrate waste solutions have been shown to produce the largest gas-generation rate; for that reason such solutions were used in this work.^{2, 3}

In a loaded full-scale column containing up to 5 MCi of ¹³⁷Cs, a dose rate of approximately 0.8 Mrad/h can be expected. Decay heat and gases produced within the body of the bed as well as inside the engineered CST particles may present special problems, especially on full-scale columns with larger hydrostatic head-pressure forces that affect gas solubility in an axial direction. Interparticle accumulated gas could potentially (1) increase pressure drop, (2) blind the surface of the CST from access to the solution, or (3) produce channels that prevent some CST from loading cesium. Additionally, intraparticle gas formation may produce uneven regional forces that may aid in particle attrition, depending on their ability to diffuse through the solution. Gas diffusivity in the saline solution within the CST micropores is impeded by solution ions, which consequently reduce the vapor pressure of the water solvent. These gases may also blind internal exchange sites that otherwise would have been available for cesium exchange with sodium. This potential effect of intraparticle gas on mass transfer inside engineered CST is unknown, but the HFIR test was expected to establish the impact. Both channeling and exchange site blinding could lead to early column breakthrough and subsequent use of more CST than planned, culminating in the need for the production of more very costly glass at the DWPF.

If not removed, hydrogen and oxygen in the proper ratios can form high-energy explosive mixtures. Therefore, movement of gases from one column to the next could produce safety concerns as well as affect the loading of the next column. Other tests at Oak Ridge National Laboratory (ORNL) using a 16-ft-tall column (as in past tests) are intended to resolve some of these concerns regarding gas disengagement.⁴

2. DESCRIPTION OF THE HFIR FACILITY

The primary mission of the ORNL reactor has been to produce radioactive isotopes, especially ²⁵²Cf and other transuranium isotopes for research, industrial, and medical applications. The extremely high neutron flux ($3 \times 10^{15} \text{ cm}^{-2} \text{ s}^{-1}$) in the central flux trap of the High Flux Isotope Reactor (HFIR) also becomes a source of neutrons for condensed matter investigations and material science studies for up to 200 international experimenters each year. Most experiments at the HFIR take place with neutrons from the reactor beam tubes rather than gamma experiments in the pool, as performed in this study.

The HFIR is a beryllium-reflected, flux-trap reactor that is light-water cooled and moderated, and uses highly enriched ²³⁵U as fuel. The fuel region is composed of two concentric elements. The inner element contains 171 fuel plates; the outer element, 369 fuel plates. The plates are curved in the shape of an involute, thereby providing a nearly constant coolant channel width. The plates in the involute are composed of a U₃O₈-Al cermet. The high-purity, aluminum-clad fuel produces high levels of ²⁴Na (15-h half-life) in the primary coolant during reactor operation and results in very high gamma fields following shutdown. Radioelements that can be expected in the pool water are ¹⁵²Eu, ¹⁵⁴Eu, and ⁶⁰Co.

The reactor core is 0.71 m (28 in.) long, with a 12.7-cm (5-in.) inner core (hole) that is also known as the flux trap. The reactor core contains 9.4 kg of ²³⁵U and 2.8 g of the burnable poison ¹⁰B. The reactor began operation at full power in 1966 at 100 MW and was later reduced to 85 MW, the level at which it operates today. The primary coolant is pumped axially through the fuel element parallel to the involuted fuel plates at approximately 13,000 gal/min.

The fuel region of the spent fuel element is surrounded by a 0.3-m-thick concentric ring of beryllium, which acts as a neutron reflector. Between the beryllium shield and the fuel element are two concentric cylinders containing poison-bearing metal to halt the reaction. The reactor reactivity is increased

as the outer cylinder plates are raised. The control plates have three axial regions containing different amounts of poison; any of these are capable of shutting the reactor down.

At a power level of 85 MW, a complete fuel cycle generally lasts for 24.7 days, depending on downtime. At 85 MW this then means that each fuel element is burned to 2100 MWd each, as evidenced by a decrease in power level. At this point, the fuel element is of little value and must be moved to the cooling pool until the gamma field has sufficiently decayed that the element can be shipped back to Babcock & Wilcox for dissolution and recycle. In the pool, the short-lived isotopes initially produce an intense gamma field that is estimated to be approximately 180 Mrad/h.^{5,6} The test in the spent fuel element did not start until after the 45th day of decay or at a dose rate of 12.4 Mrad/h gamma.

During normal operation, the temperature of the water that is present in the spent-fuel-element pool and makes contact with the reactor core vessel on the other end of the pool remains between 31 and 34EC. The spent fuel elements are stored approximately 16 ft (to the top) below the surface of the pool, while the center of the exchange column, down inside the element, was 5.4 m (17.8 ft) from the pool's surface. The center of the CST column was located at the approximate center of the active fuel region of the spent fuel element from HFIR reactor cycle no. 380.

3. EXPERIMENTAL SETUP AND OPERATION

The majority of the skid-mounted equipment used in this experiment was constructed under contract by Alloy Fabrication, Inc., of Clinton, Tennessee. The umbilical hose, adapter, outer can, and column were fabricated by various Oak Ridge machine shops. All necessary quality control tests were performed to conform to the strict guidelines of the HFIR facility as well as those of the ORNL Chemical Technology Division. All conceptual design work was performed in-house through the efforts of the ORNL Engineering Technology and the Instrumentation and Controls Divisions. Engineering drawings were prepared by the Y-12 Engineering and Drafting Section.

Because of concerns by HFIR management that a chemical spill could occur near the reactor and spent-fuel-element storage pool, the entire skid was built so that it rested upon a 4- by 4-ft, 10-in.-deep polyethylene spill-control pallet that could accommodate up to 66 gal of spillage. The simulant, coolant

water, and humidifier solutions totaled approximately 26 gal; therefore, accidental spillage became less of a concern when such a skid was used as a platform.

The skid-mounted equipment was composed of three primary sections: helium pressurization and control, chiller and column cooling, and simulant sparging and pumping systems. Each of these systems was monitored and controlled using LabView 5.1 control software running under Windows NT. The data were recorded on two hard drives, which transferred data from the primary to the backup drive at noon and midnight each day. At the end of the 7-day test, data were transferred to write-only compact disks — one copy for ORNL records and one for Savannah River.

Operation of the experiment at the HFIR required the use of mandatory alarms for certain critical parameters that were considered safety issues at the facility to avoid primarily the potential for pool contamination. A total of 11 alarms were active during the 7-day operation of the experiment. Three of these were audible alarms in the Reactor Master Control Room (RMCR), while the remainder were local alarms for the unit operator to respond to out-of-range settings. The RMCR alarms were critical to continued operation of the experiment. Any activation of these alarms for which the cause was undetermined could have resulted in termination of the experiment. A few of the alarms that are most important to the HFIR facility operations are described in general terms in this report.

The umbilical hose that carried tubing and wires to the column at the bottom of the pool was pressurized using helium gas. The pressure was specified never to drop below 8 psig. It remained nominally at 10 psig — above the hydraulic head pressure at the pool bottom — to preclude the ingress of pool water. The upper umbilical hose pressure limit was set at 11.0 psig.

The second alarm that would have activated in the RMCR was for detection of moisture inside the umbilical hose or can assembly. Dry helium gas entered the bottom of the umbilical hose and returned by way of a 1/8-in. tube placed just below the column inside the can. This gas then passed over gold-plated alumina sensors (Nyad, Inc., Martinez, California, Series 100 moisture analyzer), which were capable of detecting moisture in the gas either in units of parts per million of water or the equivalent dew-point temperature. An upper dew-point limit was set at 521EC. At or above this temperature, an alarm would sound to indicate the potential for an internal leak in the can surrounding the ion-exchange column. This moisture could have originated from a leak of cooling water or simulant solution, with very little likelihood of pool water ingress due to the umbilical hose pressurization.

The flow of dry helium at the entrance and exit of the umbilical hose was monitored using flow controllers that constantly checked the entry and exit values to determine if a gas leak were present. If the difference between the values exceeded $50 \text{ cm}^2/\text{min}$, an alarm would also sound in the RMCR and a search for the source of the leak would be required if the experiment were to continue.

3.1 EQUIPMENT

This section describes the primary pieces of equipment used in this experiment and explains their general interrelationships.

3.1.1 CST Column

The CST column was constructed primarily of 304 and 316 stainless steel (SS) with a nickel gasket on the top where the knife edges of a Parr-type closure were tightened to effect a reliable seal. The internal working space of the column was 20 cm long and 1.5 cm in diameter with the top 10 cm set aside for liquid and/or gas and the bottom 10 cm for the CST charge. At the top and bottom of this space, 200-mesh 316 SS screens were spot-welded to aid in retaining any small-size fractions of CST. Thermocouple wells (0.040 in. in diameter) passed completely through the column such that they would have been 1 cm above the bottom of a 10-cm bed and 1 cm below the top. These wells were silver soldered into the body of the steel column tube. Surrounding the column was a double wall that served as a water jacket for coolant water flowing from the bottom to the top of the column. Because of the high-radiation field, all tubing surrounding the column (shown in Fig. 1) was SS. Away from the radiation field, the coolant lines later became polyethylene. Simulant entered the column through the top and exited the bottom by way of 1/8-in. SS tubing, while 1/4-in. SS tubing was used for the coolant lines close to the column.

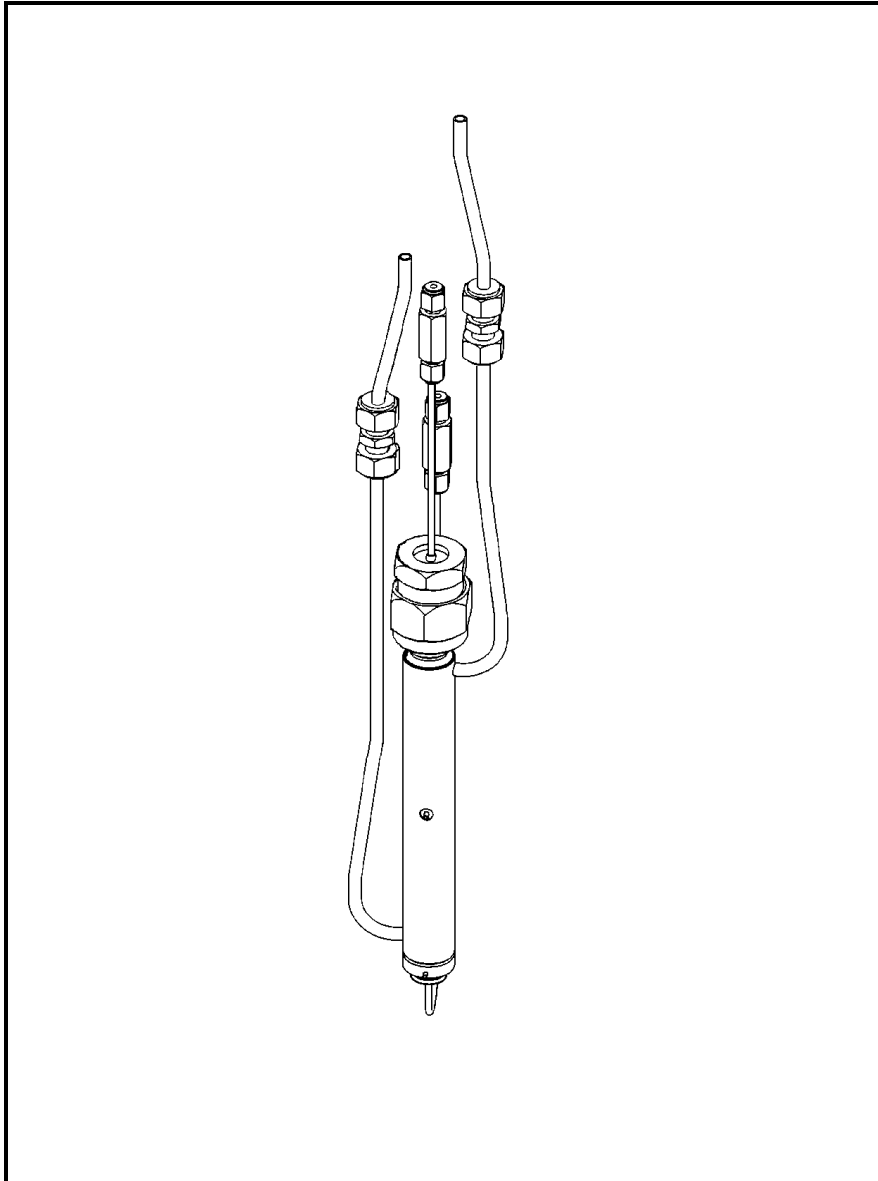


Fig. 1. CST column with attached simulant and cooling lines.

3.1.2 CST Column and Can Assembly

For an experiment to be placed inside a spent fuel element at the HFIR, procedures require the use of a secure, dimensionally exact outer can of a specified design. This can serves as a secondary barrier surrounding the experiment and receives any unintended leakage, thereby protecting the pool water and the inner environment inside the element. The outer can with the column inside is shown in Fig. 2. The SS can fits inside the 5-in.-ID opening of the spent fuel element with enough clearance to meet the HFIR guidelines. Small tabs on the side of the can (as shown) allow the centerline of the CST sorbent to be placed at the point of maximum field strength. The can is made from SS except for a high-purity aluminum gasket that joins the surfaces of the bolt head flange on top (as shown). The SS pipe above is extended at an angle away from the spent fuel element so that the Urebrade polyurethane umbilical hose attaches at a point outside the gamma field, which could effect its rapid degradation.

As shown in Fig. 2, the 1-in. umbilical hose was attached to the can extension pipe by two SS clamps. At this point, the 1/4-in. SS water-coolant lines transitioned to high-density polyethylene. It should be noted that the column and associated tubing are surrounded by the helium gas (from above) entering through the umbilical hose. As shown, a piece of 1/8-in. SS tubing is on the bottom of the can just below the column. This tubing serves to return the helium surrounding the column inside the can to the moisture monitors on the experimental skid.

To ensure that the column would remain vertical and centered, it was held in place inside the outer can assembly by a guide tube attached to the side of the column (as shown in Fig. 3). The helium return line just below the column is also more readily seen in this view. A lifting and manipulation loop can be seen welded to the top of the angled pipe above for use by HFIR operators, with tools on the end of pipe poles normally used inside the pool.

3.1.3 Column and Spent-Fuel-Element Arrangement

When the gamma-decay dose rate reached 12.4 Mrad/h (as indicated from the HFIR decay rate tables), the column and outer can assembly was placed inside the spent fuel element from reactor

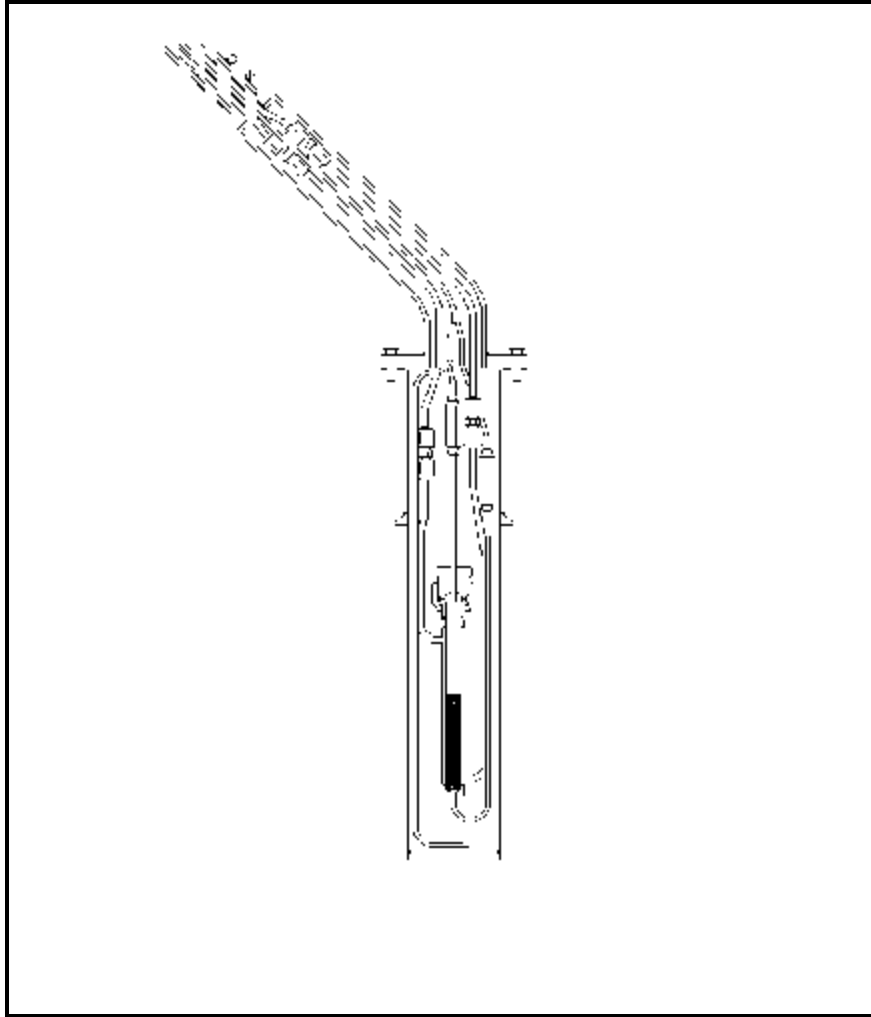


Fig. 2. CST column secured inside the standard outer can.

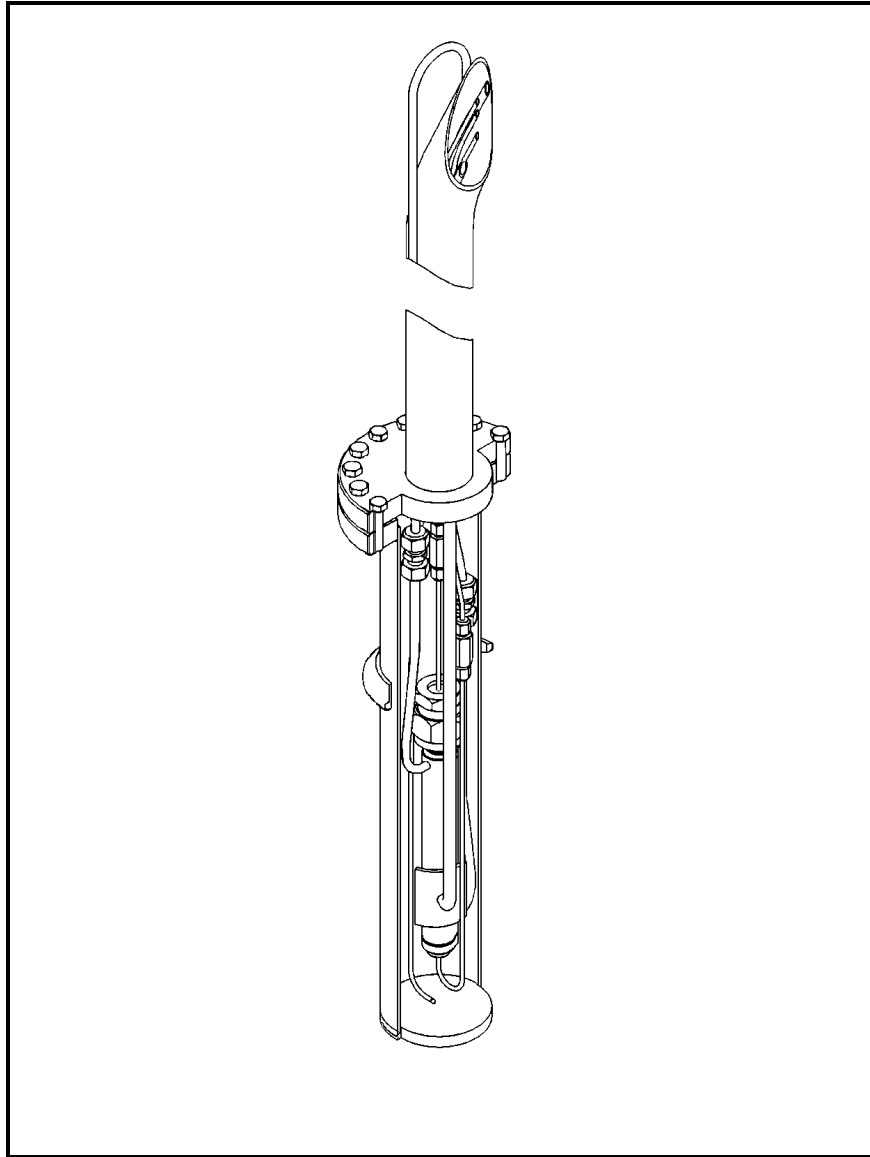


Fig. 3. Cutaway view of the column and can assembly.

cycle no. 380. The operators used their standard pool tools attached to aluminum poles to place the column and can assembly inside the spent fuel element, as shown in Fig. 4. As shown in this cross-sectional drawing, the column and can assembly rests on a cadmium post, which just makes contact with the tabs on the side of the can. It is interesting to note that the fuel centerline is 1.5-in. below that for the CST column. Because the maximum gamma dose rate actually exists above the centerline of the fuel, this situation is counterintuitive. As shown in the figure, the space surrounding the can contains the enriched uranium.

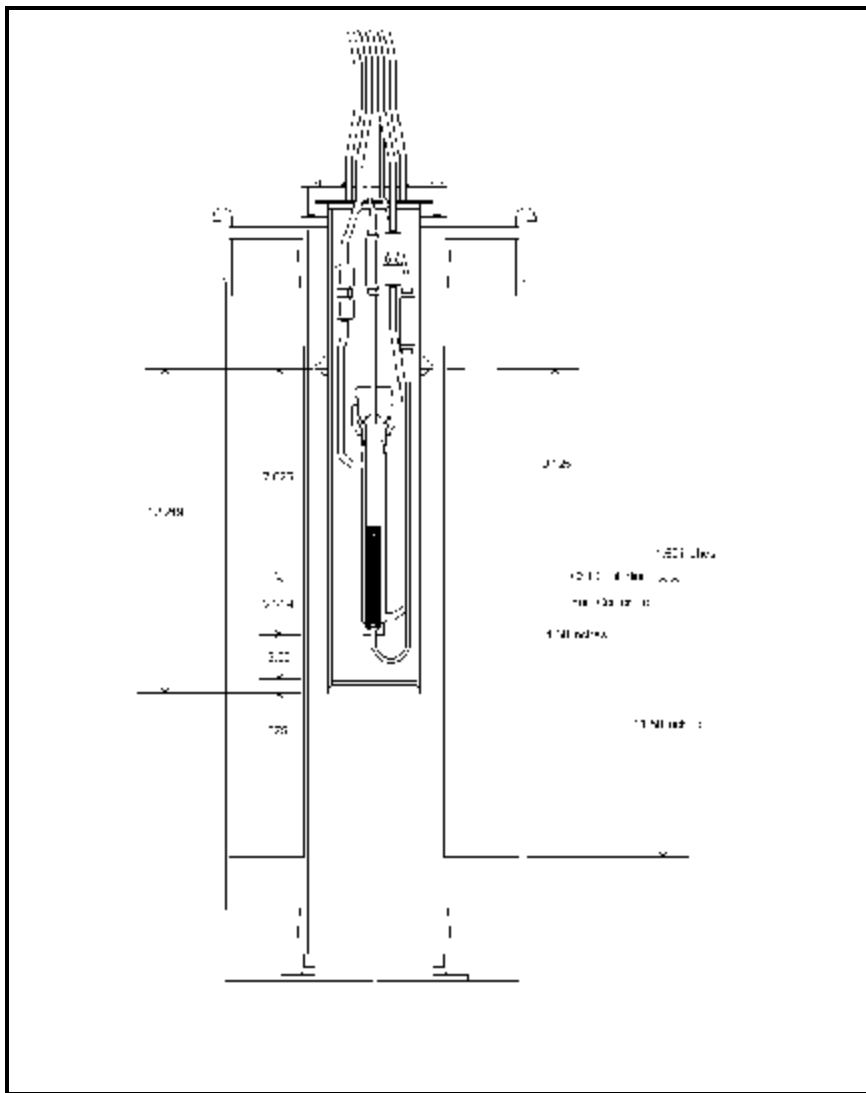


Fig. 4. Cross-sectional view of the column and can inside the spent fuel element.

3.1.4 In-Pool Experimental Setup

The centerline of the CST column was 17.8 ft below the surface of the HFIR pool, which itself is 20 ft deep, as shown in Fig. 5. At the edge of the pool, the water passed into a scupper which, as in most swimming pools, collected any floating debris. Pool water is constantly pumped through filters and mixed-bed ion exchangers to remove cations and anions. Because the nearby reactor is surrounded by the same water as that in the decay pool, the water remains thermally hot (typically between 31 and 34EC).

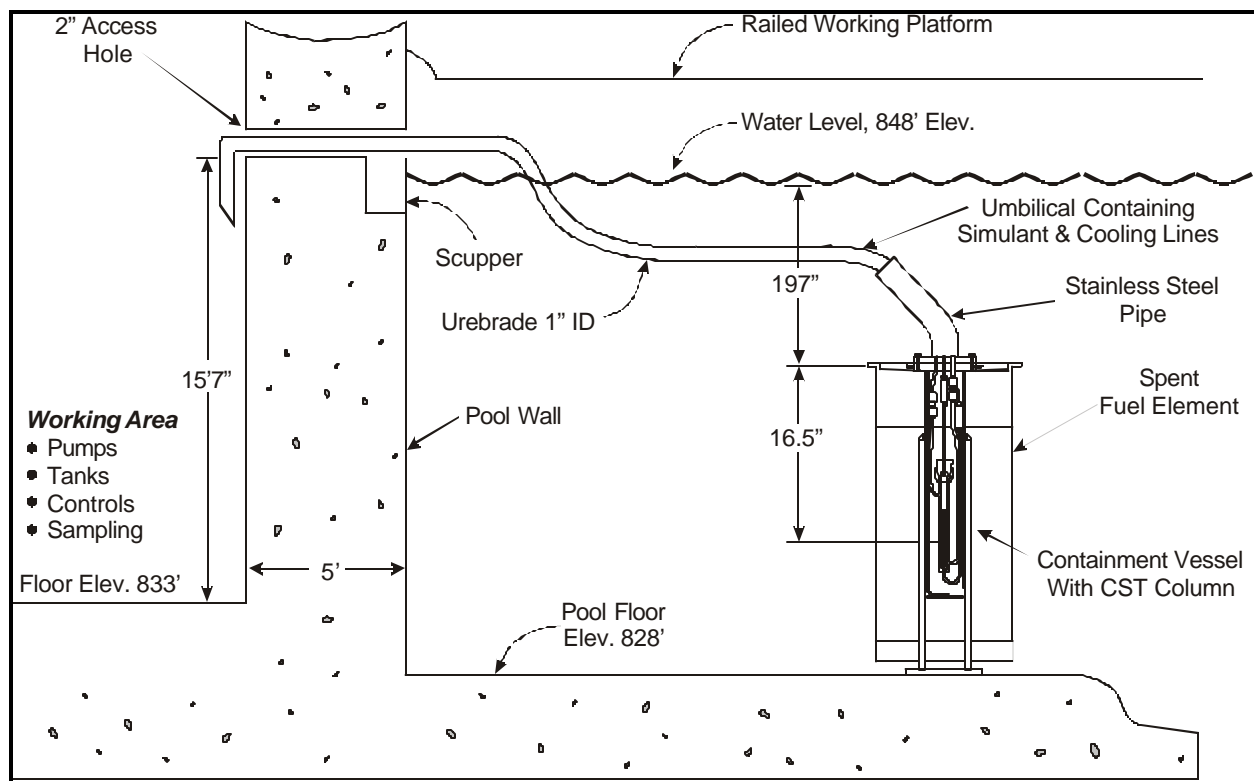


Fig. 5. In-pool experimental setup, showing the attached umbilical hose.

The wall of the pool is 5 ft thick and composed of a barite-based concrete with a 2-in.-diam access hole through which the Urebrade umbilical hose passed to connect with the experimental skid below. Within 6 in. of the surface of the pool is a railed working platform. From this platform, operators worked to remove numerous spent fuel elements during their decay cycles prior to shipment to Babcock and Wilcox

for remanufacturing. The total length of the umbilical hose originating just above the experimental skid, in what is shown (in Fig. 5) as the working area outside the wall, was approximately 40 ft.

3.1.5 Skid Configuration and Operation

The skid-mounted unit was transported to the HFIR facility and subjected to a number of electrical and helium leak tests in accordance with established quality assurance procedures. The CST column had already been prepared in the laboratory. The CST inside the column (11.10 g) remained in contact with 1.17 M sodium hydroxide solution until needed. This mass of CST resulted in a bed length of 6.28 cm. The column was bolted inside the outer can, which was attached to the Urebrade umbilical hose and transported upstairs to the pool side for placement through pool wall penetration no. 174. The end was passed through the wall and down to just above the skid. At this position, it was attached to a SS adapter coupling, where all internal tubing and thermocouples exited and connected to various parts of the unit. Prior to any other activity, the column was first pressurized to 10 psig with helium. HFIR operators lowered the column/can assembly to an empty jacket element 8–10 ft from the nearest element, where it remained temporarily at the bottom of the pool. The chiller/coolant circuit was then started.

The same procedure for column preparation and placement was followed for both the first test in the spent fuel element and the second baseline control test in the empty jacket element. For the second test, the can was opened at pool side for placement of the new column inside. Shortly after placement in the pool, the chiller/coolant circuit was started to quickly cool the column to the target temperature of 25 ± 2 EC. Therefore, the first two preliminary steps during the startup procedure always required prompt pressurization of the umbilical hose and cooling of the column followed by startup of the other skid circuits.

The following paragraphs describe the experimental skid startup procedure, operation, and control. A schematic drawing of the unit and its associated equipment is provided in Fig. 6. The startup procedure requires the sequential activation of three circuits: (1) the helium pressurization, (2) the chiller/coolant, and, lastly, (3) the simulant flow.

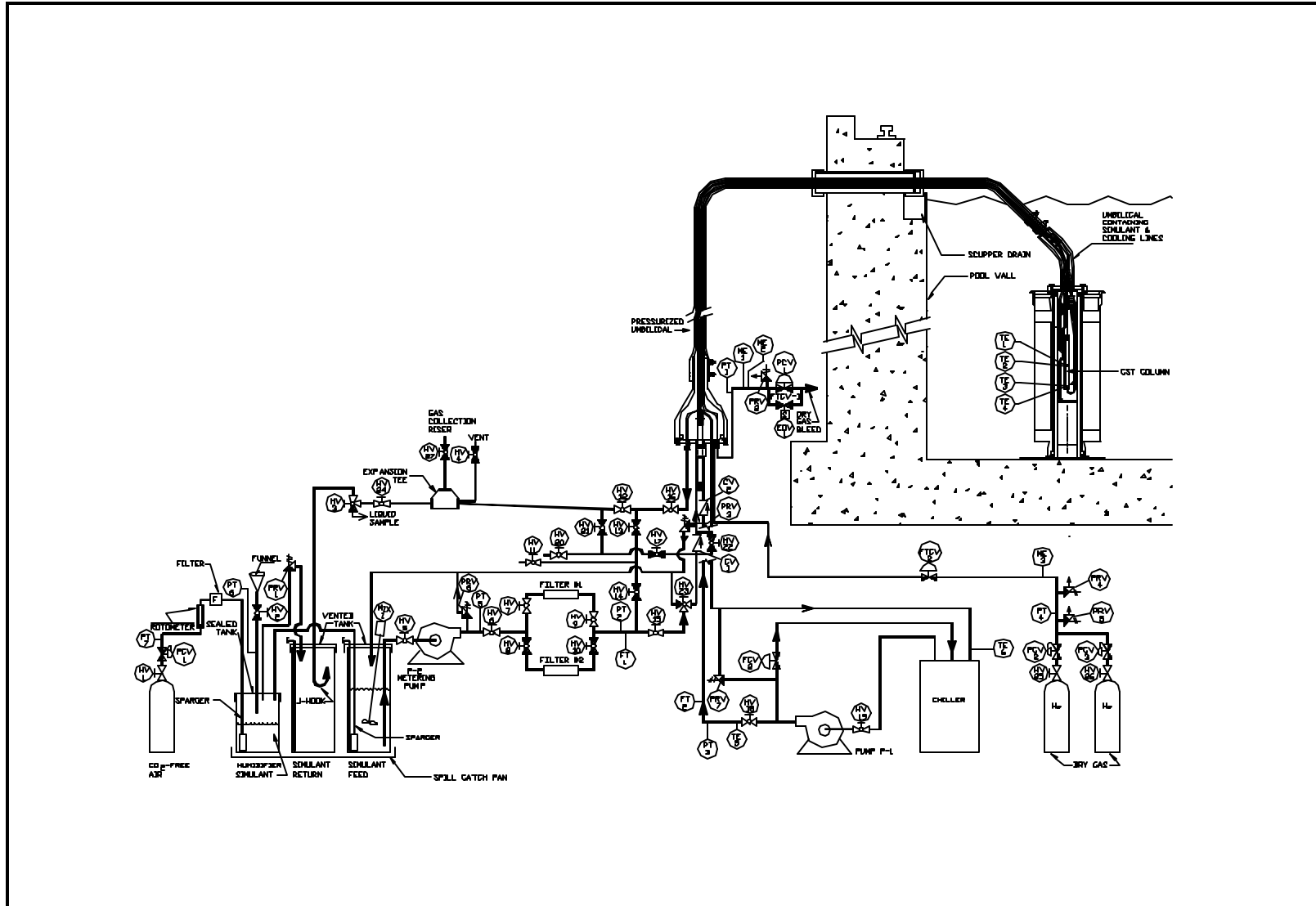


Fig. 6. Schematic of the experimental equipment layout at the HFIR pool.

The helium circuit operated with a feed pressure of 20 psig from regulated tanks near the skid. Two mass flow controllers — FTCV-1 and FTCV-2 — in the outlet and inlet lines, respectively, were used to check the difference in the incoming and outgoing volumetric flow of helium. In this way, a leak from the umbilical hose or column/can assembly can be quickly established with some confidence. Initially FTCV-2 was set at 100 sccm. During operation, the difference between the two controllers would be expected to be minimal. In this way, the volume difference in gas flow is monitored. (Pressure alone is controlled by regulators and would not by itself be a good indicator of a leak.) If the difference in values recorded by these controllers exceeds 50 sccm for more than 5 min, an alarm activates. Pressure in the umbilical hose was controlled through PT-1 near the gas exit with FTCV-1 opened or closed to maintain the target pressure in the umbilical hose at 10 psig. The data acquisition system (DAS) operated these controllers. If pressure were to drop below 8 psig, an electric solenoid valve (FTCV-1) would close completely to stop the loss of more gas and thereby temporarily maintain the pressure and sound an alarm.

The helium circuit was also used to monitor moisture exiting the column and can assembly and the full length of the umbilical hose. The dry helium gas contained less than 1 ppm moisture. The incoming moisture content was measured at moisture element ME-3. Two moisture elements measured the moisture content of the exiting helium. The dew point was displayed on a digital hygrometer, with a value of 21EC as the upper alarm limit. The two moisture elements, ME-1 and ME-2, located near the helium gas exit, were redundant, that is, one acted as a backup because of the importance of this parameter to HFIR management.

Following umbilical hose pressurization, the coolant circuit was started. A high-capacity (600- to 1000-W) chiller provided chilled water to maintain the column temperature at 25 ± 2 EC. Chiller operation was controlled by the DAS as well as a flow control valve (FCV-2), which opened and closed in order to increase or decrease the amount of water returned to the chiller sump. A positive-displacement piston pump (P-1) was used to force the chilled water through 1/4-in. polyethylene tubing located in the umbilical hose, through the column jacket, and back to the chiller sump. In addition to the temperature set point in the chiller, at a given chiller operating temperature, column temperature was regulated by controlling the amount of coolant recycle via control valve FCV-2.

Temperature was monitored inside the column using four type-K thermocouples — two at the top of the column and two at the bottom — placed 1 cm below the top and 1 cm above the bottom of the bed,

respectively. A thermocouple well passed completely through both ends of the column and the CST bed. The 0.040-in.-diam thermocouples, TE-1 through TE-4, entered the wells and met in the middle of the column. Only the top thermocouple, TE-1, was used for control of column temperature; the others were redundant. All readings were displayed at the computer console. The temperature was controlled very well using this technique, and the column target temperature was maintained.

After the helium pressurization and coolant circuits had been stabilized, the simulant pumping circuit was started. At this point, the CST in the column was covered by 1.17 *M* caustic solution. First, this solution was displaced with cesium-free simulant, which also served to displace air inside the 1/8-in. SS tubing before any cesium-containing simulant from the feed tank was pumped. Cesium-free simulant was then pumped into the column from the bottom because it was known that air could be displaced more readily in this direction. This solution was pumped sufficiently long enough to displace air in the lines and in the two groundwater filters used to prefilter simulant going to the column. When all air had been displaced from the column and from the various tubing and valves in the circuit, that part of the circuit was closed via a valve until needed.

The next step in the startup procedure was to saturate the cesium-containing simulant with CO₂-free air. The method used to ensure that enough sparging time elapsed is discussed in Sect. 4.1. First, the humidifier tank was filled with 5 gal of the simulant. The simulant feed tank was then charged with 20 gal of the simulant. The air used for sparging inside the humidifier tank passed through the alkaline solution. Upon exiting the solution, the air passed to the simulant feed tank through 1/4-in. SS tubing and simultaneously sparged the simulant solution. The small amount of CO₂ in the high-purity air used for sparging was removed in the humidifier as carbonate so that it could not pass through to the column. Additionally, air passing to the simulant feed tank was prehumidified in this way to minimize evaporation of the feed solution. This sparging continued for 4 h (as described in the following paragraphs) before the simulant feed was considered ready for use. Sparging of the solutions in this way continued throughout the entire week of the tests, with simultaneous mixing of the feed solution in the simulant feed tank.

When the feed solution was saturated with air, the valving on the skid was adjusted so that simulant that contained cesium at a target of 50 ppm could be pumped to the column for entry at the top. When ready, the simulant pump (P-2) was started by the DAS and set at a target flow rate of 6.00 mL/min. Solution passed through one of two 0.45- μ m groundwater filters (GWV lot no. 18440, Gelman

Sciences) and then to the column. The flow rate was adjusted by the DAS, based on signals from a factory-calibrated RheothermTM metering apparatus with a low-flow-rate alarm set at 5 mL/min and a high-flow-rate alarm at 8 mL/min. The flow rate remained very constant, varying only slightly from the target flow rate over the duration of both tests.

Simulant exiting the column passed from the umbilical hose through the adapter and then flowed to a gas-collection column made from clear polyvinylchloride (PVC) and calibrated along its side. The effluent solution in the returning column was allowed to fill the vertical column until it overflowed from the top, at which time a valve was closed. A side arm parallel to the column and originating from the bottom of the column was used to equilibrate the gas volume in the collector with atmospheric pressure just prior to taking a gas reading. The gases from the column rose inside the collector, and the liquid effluent exited at the bottom. The column effluent passed a sampling valve and then flowed to a 30-gal simulant return tank.

The total volume of effluent passing the sampling valve was constantly integrated based on data from the RheothermTM and clock time and was recorded at each liquid sampling of 12 mL of effluent. Column effluent was removed every 2 h. Care was taken to allow new sampling solution to displace solution in the 1/8-in. tubing near the valve to avoid cross-contamination from a previous sample. Every second sample removed was submitted for chemical analysis of its cesium content. The test continued for 168 h. The same startup procedure was employed for both the baseline (control) test and the test in the spent fuel element.

3.2 DEVIATIONS FROM THE ORIGINAL TECHNICAL TASK PLAN

The work documented in this report was originally described under an Office of Technology Development Technical Task Plan No. ORO-8-SD-11.⁷ However, a number of calculations and computer modeling performed during the course of preparation for work at the HFIR facility dictated some changes to the planned operating conditions. Most changes were made to ensure that complete cesium breakthrough curves were obtained or that conditions were near optimum to facilitate the maximum generation of radiolysis gas.

Originally, the cesium concentration in the feed simulant was 19 ppm. This level was increased to 50 ppm to ensure that the full breakthrough curve was observed within the test duration. In addition, the silicate component of the simulant was omitted to prevent the plugging of CST pores that sometimes occurs with this problematic chemical species in simulant.

Modeling of column operation, together with gas generation calculations, revealed that the simulant flow rate and resulting superficial velocity should be lower to permit adequate residence time of simulant in the radiation field to produce gas. The original simulant flow rate was decreased from 7.25 to 6.00 mL/min, with resulting superficial velocities decreasing from 4.1 to 3.4 cm/min.

The original column bed height was to be 10 cm, which would have required 17.1 g of CST charge. However, due to a communications error, both columns were instead charged with 10 cm³ (11.1 g of CST), yielding a bed height of 6.28 cm. This unintended deviation from the standard bed size used in most previous laboratory tests did not affect the results of this study.

4. MATERIALS AND METHODS

The CST used in these column-loading tests was a commercial product that has been described in detail elsewhere.^{8, 9} This granular sorbent, IONSIV IE-911®, was produced by UOP, LLC, of Mt. Laurel, New Jersey, from a chloride-based process in 1998 and has a designation of lot no. 999098810005 CST (98-5). Both wet and dry screenings of this batch were performed and showed an average particle size of 410–437 µm (as received) and 412–457 µm following caustic pretreatment. The higher values in the latter range result from the wet-screen sizing, in which swelling was reported between 7 and 11%.

Taylor reports a K_d value for cesium from this batch of CST from high-nitrate simulant at 24EC of 1406 L/kg (based on a dry weight at 400EC) and 1300 L/kg (using a dry weight at 105EC).⁹ Additionally, a weight loss of 6.5% was measured upon drying at 105EC for 2 days and 15.4% after 4 h at 400EC.

The CST (98-5) was weighed (11.1 g) into a beaker. Excess fines were removed using 1.17 *M* caustic with swirling and decantation. Using the same caustic solution, the CST was washed into the SS column (1.5-cm diam by 20-cm length) and then pretreated by pumping 1.17 *M* caustic solution in the

bottom-up mode at 6 mL/min for 24 h in a once-through pretreatment scheme. This caustic concentration stabilized the CST since it has the same molarity as in the high-nitrate simulant and is that specified in the standard pretreatment procedure.¹⁰ The column was then sealed, and the resulting 6.28-cm-high bed remained in contact with this solution. The column remained in an upright position until it was transported to the HFIR site for installation into the primary outer can. In addition to attached simulant lines, the CST bed and the empty space above it (13.7 cm) remained filled with the caustic solution. In this way, these areas remained free of air that would need to be displaced during the startup of our tests. Based on prior experience, the wet bed of CST was expected to have a liquid-filled, bulk porosity of 50 vol %. The same CST sorbent and pretreatment method were employed for material used in both the baseline and the hot gamma- loading tests in the spent fuel element.

4.1 SIMULANT SATURATION PARAMETERS

Since the residence time of the high-nitrate simulant pumped through the column apparatus and bed in the gamma field at the targeted flow rate of 6.00 mL/min was only 5.3 min, it was important to ensure that conditions were conducive to radiolytic gas bubble formation.¹¹ Within this period of time, sufficient radiolytic gases would have to be produced to potentially have some effect on column performance.

Solubilities of oxygen, nitrogen, and hydrogen gases were known from work performed at Hanford on similar solutions (241-SY-101 simulated waste). These values were corrected using the Schumpe model for activity differences in temperature and sodium content.^{11,13} In conjunction with corrected gas solubilities, G-values for these gases were derived by Walker at Savannah River using CST-free 5.6 M high-nitrate simulant alone, as well as in the presence of the CST IONSIV™ IE-911 slurries.^{2,11} Based on these data, calculations, and tabulated gamma dose rates for the HFIR spent fuel elements, it was decided to ensure that the simulant was presaturated with respect to atmospheric gases prior to being pumped to the column. In this way, we conservatively take credit for the simulant already being saturated at 1 atm of pressure.

In order to accomplish this presaturation, CO₂-free air was first sparged inside a sealed acrylic tank containing approximately 5 gal of simulant which, since it is alkaline (1.2 M OH⁻), will aid in removing the

small amount of remaining CO₂ as carbonate and also prehumidify the exiting gas. The exiting, prehumidified, CO₂-free air then passed to a 30-gal polyethylene tank containing 20 gal of simulant, where it was constantly mixed and sparged by the air from the humidifier tank. All sparging took place through 0.4- μ m SS sintered metal spargers, which produced a very fine bubble froth in each tank.

Prior to implementing this sparging procedure in the field, it was necessary to determine how long it would take to achieve saturation. The mixing propeller energy input, temperature, propeller speed, and sparging rate and time became important parameters that required testing at the same time the dissolved oxygen content was measured. These tests were performed on the bench top at Savannah River as well as at ORNL inside the unit during early equipment checkout. Tests at Savannah River showed that the use of simulant or water yielded comparable results; therefore, tests with the unit at ORNL employed water.

The sparge time needed to saturate the solution with oxygen from air was measured using a fiber-optic oxygen sensor that operates in both gas and liquid phases and is unaffected by alkalinity and high salt content.¹⁴ These solution conditions precluded the use of a YSI™-type dissolved oxygen apparatus, which would have resulted in membrane dissolution. The apparatus used was purchased from Ocean Optics and employed a fiber-optic oxygen probe that measured oxygen content via fluorescence quenching on an immobilized ruthenium complex. Mass transfer coefficients and sparge-time constants were derived from a number of tests in which helium was first used to remove all oxygen from the mixed solution and air was then sparged until steady-state oxygen saturation was approached. The calculated mass transfer coefficient of 4.2×10^{14} /s was obtained and corresponded to a sparge time constant of 39.7 min.¹⁴ The time to steady-state saturation is approximately three times the calculated time constant or 120 min for a gas flow rate of 200 cm³/min and a mixer speed of 400 rpm. Due to the absence of baffles in the simulant feed tank, the system was estimated to be 50% efficient.

Because it was important that the simulant be saturated with respect to atmospheric gases, the sparging time was doubled (from the calculated 2 h to 4 h) prior to pumping simulant to the column. Air sparging and mixing continued in this way for the full 7-day duration of both HFIR tests.

4.2 PRELIMINARY PUMPING TESTS

During the construction phase for the experimental skid and associated equipment, a series of pumping tests was performed to determine the expected pressure drop through 80 ft of 1/8-in. SS tubing. It was expected that this same amount of tubing and test configuration would be used at the HFIR pool. Two connected loops of tubing were strung overhead and attached to a scaffold with 15.5 ft of rise initially and then 17.0 ft to the floor in the last loop. This arrangement was to approximate pumping up the side of the HFIR pool wall, through the wall, and down to the column in the pool — and then back. High-nitrate-based simulant was pumped through the tubing using a positive-displacement piston-head pump (ACCU SciLog, Middleton, Wisconsin, with an ACCU FM-40 RHOOSKY head with 450-rpm drive). The head on this pump would later be changed to a gear-drive type (Micropump, Vancouver, Washington, Model 184-000-010) for use on the experimental skid at the HFIR.

During startup of the pump, the back pressure was displayed by a calibrated pressure transducer and also by a calibration gauge as a secondary check. The initial back pressure increased to 7.5 psig as the solution moved up the first leg of tubing and then fell to approximately 2.5 psig as the solution flowed downhill. The back pressure then rose to 8.7 psig as it moved up the second leg; this sequence represented the movement from the column at the bottom of the pool back to the top of the pool wall. On the last leg of tubing, the pressure dropped as solution moved downward (as it would outside the pool to our skid below) and settled at a back pressure of approximately 2.5 psig at steady state for as long as pumping continued.

During actual operations at the HFIR pool facility, the back pressure of simulant through the 1/8-in. SS line remained nearly constant at approximately 5 psig, as displayed at PT-5. Coolant water pumped through 1/4-in. polyethylene tubing that was parallel to simulant tubing, had less internal resistance to flow to the column and back, and constantly displayed a back pressure of 0.9 to 1 psig at PT-3. These values are significant because — at the very low back pressures experienced in both the pumping tests and at the pool side — bubble formation was predicated only upon overcoming approximately 1 atm of pressure, rather than the 1.5 atm existing inside the column under 17.8 ft of water head. Without this benefit, gases that exceeded the higher total pressure at depth might not have been able to form and exit the solution, thereby compromising the success of the experiment.

5. ANALYTICAL METHODS

This project has relied on four analytical methodologies directed at identifying the compositions of the high-nitrate simulant waste feed and column effluent solution and performing a final analysis of collected radiolytic gas. Most methods employed are traceable to accepted U.S. Environmental Protection Agency (EPA) SW-846 test procedures and guidance that are needed to ensure compliance with the Resource Conservation and Recovery Act, Public Law 94-580, as amended.¹⁵ All samples submitted for chemical analyses were accompanied by chain-of-custody documentation that was signed off by relinquishing and receiving staff with specific tracking numbers to ensure proper sample and analysis control in accordance with ORNL guidelines. Additionally, to minimize preparation differences in concentrations, the high-nitrate simulant feed solution was prepared as one large batch and then split in half for use in both the baseline test and the hot test inside the spent fuel element. After aging for 48 h and filtration through a 0.5- μm polypropylene filter (Betafine-D™, CUNO Inc., Meriden, Connecticut), the simulant was ready for use. This solution was then sampled for chemical analysis just prior to transport to the HFIR facility.

5.1 SIMULANT FEED AND COLUMN EFFLUENT

Simulant feed solution was analyzed for cations by inductively coupled plasma (ICP) analysis, using a Model 61E Trace ICP from Thermo Jarrell Ash as specified in EPA method SW846-6010B, “Inductively Coupled Plasma–Atomic Emission Spectrometry,” Revision 2, December 1996. This method analyzes multiple elements using sequential or simultaneous means. Accuracy was maintained using National Institute of Standards and Technology standards. The high-nitrate simulant was analyzed using nitric acid following a microwave pressure digestion. The resulting cation data are presented in Table 1.

Table 1. Composition of high-nitrate simulant used in CST tests

Component	Target concentration (<i>M</i>)	Analytical concentration(<i>M</i>)
Na ⁺	5.6	5.6 ^a
K ⁺	0.0041	0.0045
Cs ⁺	0.00038 (50 ppm)	0.00039 (52 ppm)
OH [†]	1.17	NA ^b
NO ₃ [†] (total)	2.84	2.84
NO ₂ [†]	0.37	0.38
AlO ₂ [†]	0.32	0.32
CO ₃ ^{2†}	0.16	NA ^b
SO ₄ ^{2†}	0.22	0.20
Cl [†]	0.040	0.039
F [†]	0.050	0.050
PO ₄ ^{3†}	0.010	0.011
C ₂ O ₄ ^{2†}	0.008	NA ^b
MoO ₄ ^{2†}	0.0002	0.0002

^aCalculated from solution density at 22EC (Ref. 16).

^bNot analyzed.

Column effluent samples, removed every 2 h during testing, were analyzed for their cold cesium (¹³³Cs) content by ICP–mass spectrometry in accordance with method SW846-6020, “Inductively Coupled Plasma-Mass Spectrometry,” Revision 0, September 1994. This method of analysis can be applied to over 60 elements, with detection limits generally below 0.02 µg/L (ppb) for simple matrices. Typical detection limits from nitrate-based matrices in the range of 2 to 4 *M* are 10 ppb with an error bar of ± 10% due to the need for an initial large dilution of 1:10,000, which is responsible for the quoted probable error. A detection limit for ¹³³Cs from a simple matrix requiring no dilution is stated as 10 ng/L (ppt).

Primary anions comprising the high-nitrate simulant were analyzed in accordance with method SW846-9056, "Determination of Inorganic Anions by Ion Chromatography," Revision 0, September 1994.¹⁵ Generally, minimum detection limits are in the range of 0.05 mg/L for F⁻ and 0.1 mg/L for Br⁻, Cl⁻, NO₃⁻, NO₂⁻, PO₄³⁻, and SO₄²⁻. Due to dilution error, results quoted for anion concentrations are ± 10%. The anion concentrations of the simulant feed solution are also presented in Table 1.

5.2 RADIOLYTICALLY FORMED GASES

Gases associated with the test performed inside the gamma field of the spent fuel element originated from two sources: those purposely dissolved in the saline simulant feed to saturate or supersaturate it with respect to CO₂-free atmospheric gases and those produced as a result of gamma radiolytic splitting of water to form hydrogen and oxygen gases. These gases were collected as they exited the column in a vertical gas-collection tube filled with simulant that was displaced by the incoming gas. Gas was removed by attaching a double-valved, preevacuated steel sample bottle that was used to evacuate the gases for transport to the Analytical Chemistry Laboratory at the Oak Ridge Y-12 facility. Liquid was allowed to flow into the bottom of the gas-collection column as gases were withdrawn to prevent solution degassing.

The Mass Spectrometer Laboratory, located at the Oak Ridge Y-12 facility, used a method referred to as Y-P65-6011. The instrument used was a Model VG (Vacuum Generator) 3001 ISOTOPES mass spectrometer, manufactured in Winsford, England. This model is a magnetic sector instrument as opposed to the common quadrupole type. Gas compositions were reported in volume percent and included an analysis of local air, with reported 1% standard deviations; these data are reported in Table 2 in Sect.6.

6. RESULTS

6.1 RADIOLYTIC GASES

Initially, a Lexan gas-collection column was used, but this column presented problems during operation and had to be replaced with another. This change was accomplished in less than 1 h, while the system continued to operate. The new column was made from clear PVC pipe with SS end caps and was found to be superior to the Lexan column, which formed stress cracks from embedded fittings. The new PVC column operated during the last 101 h of the test, between hours 67 and 168. The gamma dose rates between these two times were 11.6 and 10.4 Mrad/h, respectively. The changing gamma dose rate inside the spent fuel element at the centerline can be represented by $\text{Mrad/h} = 12.4 e^{-0.000924T}$ for $T = 0$ to 168 h; the rate starts at 12.4 Mrad/h at $T = 0$ and is down to 10.4 at $T = 168$ h. Upon integrating between $T = 67$ h and 168 h, the gamma dose to the column during this gas collection period was 1124 Mrad of gamma.

At the end of the test, the total volume of gas collected in the gas-collection apparatus was 90 mL. Unfortunately, this volume contained not only the radiolytic gases but also air that entered the system accidentally when the direction of flow of simulant was reversed in an effort to determine if any gases were held back in the column. The air entered through an open valve in the vicinity of the gas-collection column on the unit.

The 90 mL of gas collected was measured at 1 atm. Opening a valve next to the gas-collection column to equilibrate it momentarily with atmospheric pressure resulted in no change in level inside the column. The gas was collected as previously described and submitted for mass spectrometry analysis. The results of the gas analysis — in addition to those for a standard air sample — are presented in Table 2.

Since the radiolytic gas is contaminated by air, it is necessary to determine the precise amount of radiolytic gas alone. To do this, one must assume that any nitrogen present has come from air, an assumption that is justified based on past studies.^{2, 12} Walker has shown that N_2O can form, probably from nitrite or nitrate, but that nitrogen (an even more reduced form of the oxide) is much less favorable thermodynamically. As shown in Table 2, only a trace amount of mixed oxides of nitrogen (0.001%) was measured. Walker has reported production of 2.3% N_2O upon irradiating a CST slurry in a 1-Mrad/h gamma field.² Therefore, we know that the primary radiolytic gases of interest will be hydrogen and oxygen, with nitrogen and argon originating from the air. Additionally, since air contains only traces of hydrogen (0.003%, Table 2), we can assume with some confidence that the hydrogen present has come from gamma radiolysis of the simulant water.

From the analysis of the air standard in Table 2, we can determine the amount of radiolytic oxygen volume from the fixed volumetric ratio of nitrogen to oxygen in air (3.851). We can conclude that of the 90 mL gas total, 15.35 mL of oxygen came from air. Therefore, the difference (9.54 mL) came from radiolysis. Since 5.48% of the column gas was hydrogen, then 4.93 mL of

Table 2. Gas analyses by mass spectrometry

Gas	Composition (vol %)	
	Local air	Gas column analysis ^a
Xe	<0.001	<0.001
Kr	<0.001	<0.001
CO ₂	0.06	0.005
Ar	0.98	0.61
O ₂	20.36	27.66
N ₂	78.4	65.68
H ₂	0.003	5.48
He	<0.01	0.17
CH ₄	0.003	0.008
CO	<i>b</i>	0.08
Ne	<i>b</i>	0.003
NO _x	<i>b</i>	0.001
C ₂ H ₆	<i>b</i>	0.003
H ₂ O (est.)	<i>b</i>	0.3

^aThe column contained a total of 90 mL of both radiolysis gases and some air leakage.

^bNot detected.

hydrogen was produced, for a total volume of radiolysis gas of 9.54 mL O₂ plus 4.93 mL of H₂, or 14.48 mL over the last 101 h of gas collection at a simulant flow rate of 6 mL/min. This would mean that 0.398 mL of radiolytic gas per liter of simulant pumped was produced on this basis. The volume of total radiolytic gas expected during 101 h (and, therefore, the gas-generation rate) is in line with the calculations of Walker, who expected approximately 0.4 mL/L during this period of the test.²

6.2 CESIUM BREAKTHROUGH CURVES

Over the duration of both the radiological test (i.e., inside the intense field of the spent fuel element) and the baseline test nearby (i.e., away from the radiation field), which were conducted under identical operating conditions, effluent from the columns was removed every 2 h. Every second sample was submitted for cesium analysis by mass spectrometry. The fractional amount of cesium in the column effluent compared with the feed concentration (52 ppm) is plotted against time in Fig. 7. In addition to the radiological and baseline breakthrough curves, that of the VERSE model is also plotted for comparison. The VERSE model takes into account parameters such as starting cesium concentration, bed height, flow rate, and superficial velocity of simulant.

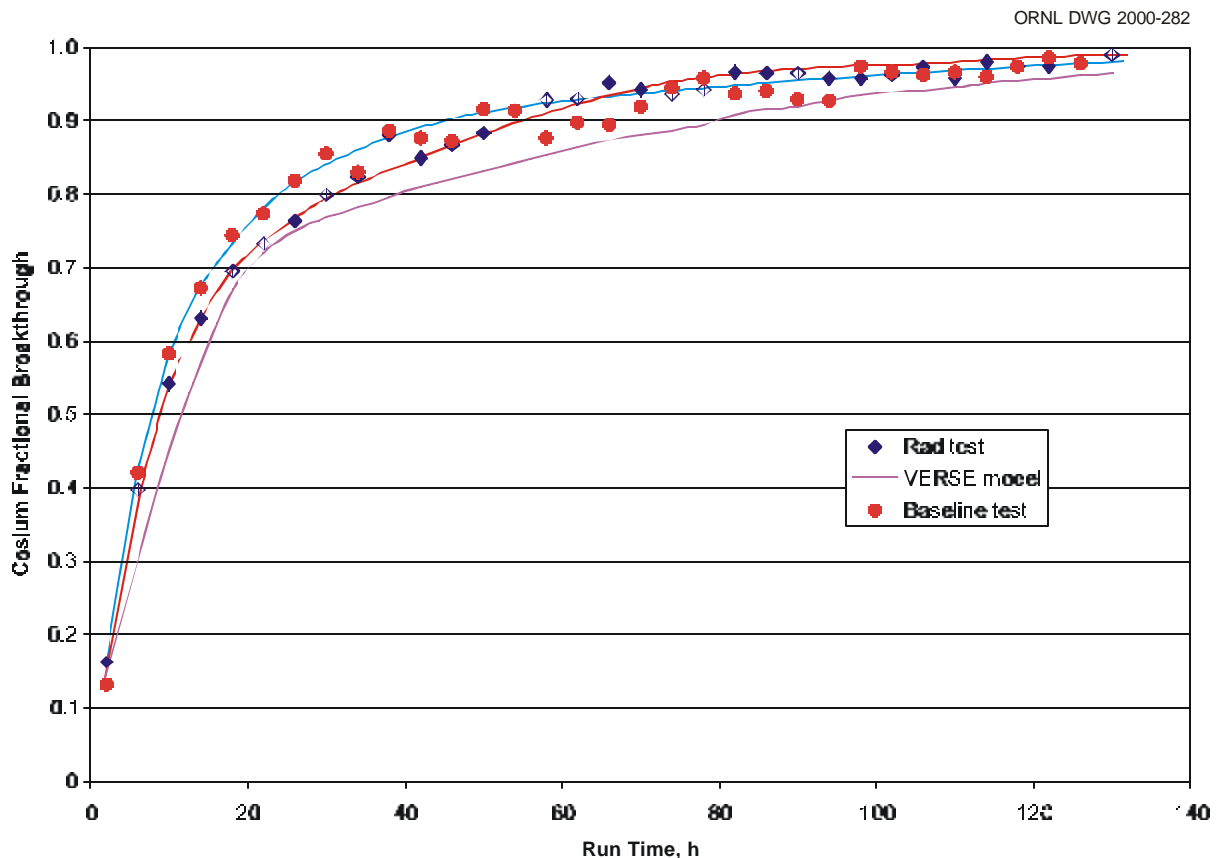


Fig. 7. Cesium fractional breakthrough curves.

One immediately sees that the shapes of the curves deviate from those in which scale and exchange kinetics produce a mass transfer zone shorter than the length of the column. Such curves normally have

a more sinusoidal appearance. In this simulant and with this CST, the mass transfer zone is “substantially” longer than the column and is actually measured in feet.

Within the quoted analytical error of mass spectrometry, the breakthrough curves for the radiological test and the baseline control test performed in the absence of the gamma field are identical, with detection limits quoted at 10 ppb in our high-nitrate matrix. Because the curves are essentially the same, one may conclude that the radiolytic gas formed in the 12.4- to 10.4-Mrad/h gamma field during cesium loading, compared with an expected dose rate in the field of 0.8 Mrad/h, had no observable effect upon cesium-loading kinetics. Changes in the shape of the curves due to exchange-site blinding inside micropores, column short-circuiting, or CST interparticle hydraulic macroeffects are not apparent.

6.3 CST X-RAY SPECTRA

During the 168-h period that the CST was inside the intense gamma field of the spent fuel element, it would have received a total dose of 1,930 Mrad. That part of the energy absorbed by the crystalline fraction of the CST could potentially produce a change in the crystal lattice. To investigate the potential and magnitude of such a change, the following X-ray spectral scans of the CST removed from the spent fuel element and those for the unirradiated starting material are shown in Fig. 8.

The X-ray spectra in Fig. 8 indicate that some minor change has taken place in the CST exposed to the gamma field (top spectrum) compared with the unirradiated baseline control sample. The area between 17 and 25E shows the most change. A few scattered variations in peak intensity at a few other angles are also observed; however, no attempt has been made to index these very minor changes. These changes may reflect dislocations in the CST lattice due to absorbed and stored energy.

7. CONCLUSIONS

Tests in which cesium was successfully loaded onto CST-containing columns in ORNL’s HFIR spent-fuel-element storage pool were performed under closely controlled conditions to take advantage of the high gamma dose rates present inside reactor spent fuel elements. These elements provided a uniquely suitable and conservatively intense source of gamma radiation capable of forming potentially problematic

radiolytic gases inside CST micropores and bulk column solution during loading. Radiolytic gas composed of oxygen and hydrogen (66% O₂, 34% H₂) was formed

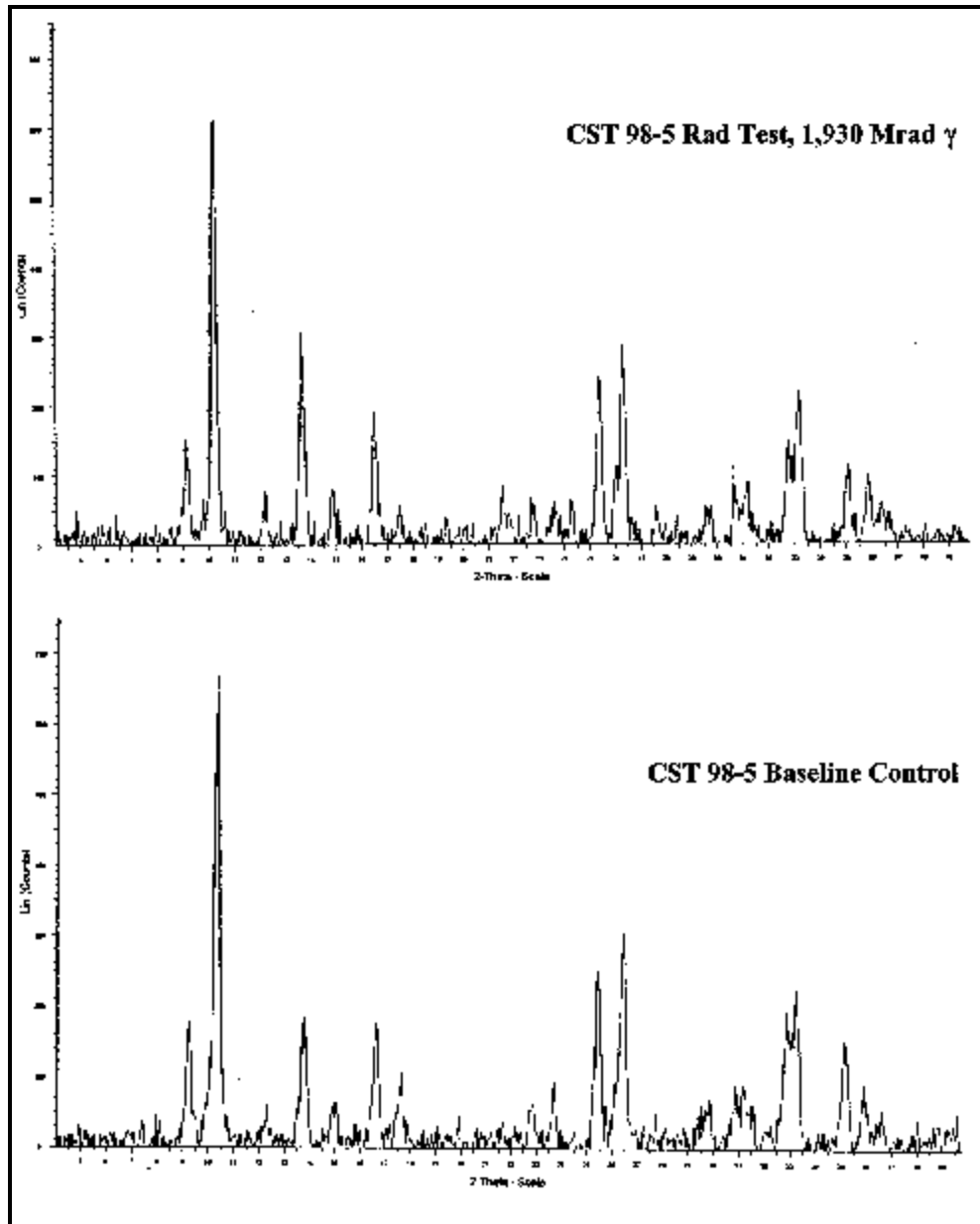


Fig. 8. X-ray spectra of irradiated and unirradiated CST.

inside the exchange column at a previously calculated generation rate of 0.4 mL/L in high-nitrate simulant. Gases formed during the loading of cesium onto the engineered 98-5 CST in the gamma

field of the HFIR spent fuel element, at dose rates ranging from 12.4 to 10.4 Mrad/h over a 168-h period, had no observable effect upon column loading or operation. Cesium breakthrough curves for both the irradiated test and the control test (i.e., that conducted in the absence of radiation) were shown to be identical and were in good agreement with the VERSE computer-generated curve. Results conclusively indicate that even upon performing the column loading in an intense radiation field expected to be nearly 16 times that encountered in an actual field-loaded column, no operational problems stemming from interparticle or intraparticle gas should be expected.

8. ACKNOWLEDGMENTS

The authors gratefully acknowledge the contributions of the following technicians who assisted with the operation of the test unit at the HFIR facility over the various shifts: Kim Anderson, Bob Cummins, Betty Evans, Jim Hewitt, Hal Jennings, Robert McMahon, and Jim Travis. A special thanks is extended to the staff of the Engineering Technology Division's Irradiation Engineering Group headed by Ken Thoms, who, together with coworker Dennis Heatherly, performed most of the design and oversaw construction of the column/can assembly and the umbilical hose section, which were key components in these experiments. HFIR's Experiment Coordinator Randy W. Hobbs provided many hours of close support on every phase of this project's development, in addition to helping facilitate its approval process through numerous review committees. We also wish to thank the staff of the Research Reactors Division for allowing us to run our tests in their pool during especially "busy times." The authors also recognize the work of both ORNL and Savannah River Technology Center (SRTC) Instrumentation and Controls support staff, who put many hours into the testing of control software and hardware, thereby ensuring that the test unit operated as well as it did. SRTC personnel spent many days away from their home while working on-site in an effort to ensure the success of these tests.

9. REFERENCES

1. H. Harmon, S. Schlahta, T. Kent, D. Wester, K. Rueter, and S. Fink, *Tank Focus Area Savannah River Site Salt Processing Project Research and Development Program Plan*, PNNL-13253, Rev. 1, Pacific Northwest National Laboratory, Richland, Washington, November 2000.
2. D. D. Walker, *Radiolytic Gas Generation in Crystalline Silicotitanate Slurries*, WSRC-TR-99-00285, Rev. 0, Westinghouse Savannah River Company, Aiken, South Carolina, September 17, 1999.
3. K. J. Rueter and S. F. Piccolo, *Position Paper on Performance of Small CST Column Gas Generation Test in Radiation Field*, HLW-SDT-99-0257, Rev. 0, Westinghouse Savannah River Company, Aiken, South Carolina, August 30, 1999.
4. T. D. Welch, K. K. Anderson, D. A. Bostick, T. A. Dillow, M. W. Geeting, R. D. Hunt, R. Lenarduzzi, A. J. Mattus, P. A. Taylor, and W. R. Wilmarth, *Hydraulic Performance and Gas Behavior of a Tall Crystalline Silicotitanate Ion-Exchange Column*, ORNL/TM-1999/103, Oak Ridge National Laboratory, Oak Ridge, Tennessee, February 2000.
5. M. W. Kohring, *Gamma Flux Measurements on Spent High Flux Isotope Reactor (HFIR) Fuel Assemblies*, ORNL/CF-86/256, Oak Ridge National Laboratory, Oak Ridge, Tennessee, August 7, 1986.
6. M. W. Kohring, ORNL, to R. E. Jones, ORNL, "Spent HFIR Fuel Assembly Dose Rates," Internal Correspondence, Oak Ridge National Laboratory, Oak Ridge, Tennessee, September 4, 1987.
7. "Modular Evaporator and Ion Exchange Systems for Waste Reduction," Subtask C6: Gas Generation Impacts, Rev. 01, Technical Task Plan no. ORO-8-SD-11, 3GBT, Office of Technology Development, September 26, 2000.
8. D. A. Bostick and W. V. Steele, *Thermal and Physical Property Determinations for Ionsiv IE-911 Crystalline Silicotitanate and Savannah River Site Waste Simulant Solutions*, ORNL/TM-1999/133, Oak Ridge National Laboratory, Oak Ridge, Tennessee, August 1999.
9. P. A. Taylor and C. H. Mattus, *Thermal and Chemical Stability of Crystalline Silicotitanate Sorbent-Interim Report*, ORNL/TM-2000/307, Oak Ridge National Laboratory, Oak Ridge, Tennessee, September 29, 2000.

10. D. D. Walker, *Pretreatment Guidelines*, SRT-LWP-2000-0028, Rev. 0, Westinghouse Savannah River Company, Aiken, South Carolina, March 3, 2000.
11. R. A. Jacobs, Westinghouse Savannah River Company, to J. T. Carter, Westinghouse Savannah River Company, "HFIR Gas Generation Estimates," Interoffice Memorandum, HLW-SDT-2000-00249, Rev. 0, June 22, 2000.
12. J. D. Norton and L. R. Pederson, *Solubilities of Gases in Simulated Tank 241-SY-101 Wastes*, PNL-10785, Pacific Northwest Laboratory, Richland, Washington, September 1995.
13. T. Hang and D. D. Walker, *Gas Generation and Bubble Formation Model for Crystalline Silicotitanate Ion Exchange Columns*, WSRC-TR-2000-00177, Rev. 0, Westinghouse Savannah River Company, Aiken, South Carolina, June 16, 2000.
14. B. B. Anderson to S. Fink, "Trip Report and Results of ORNL HFIR Sparge Test," SRT-ADS-00-0375, Westinghouse Savannah River Company, Aiken, South Carolina, August 15, 2000.
15. *Test Methods for Evaluating Solid Waste, Physical/Chemical Methods*, SW-846, Rev. 2, U.S. Environmental Protection Agency, Washington, D.C., September 1994.
16. D. D. Walker, *Preparation of Simulated Waste Solutions*, WSRC-TR-99-00116, Rev. 0, Westinghouse Savannah River Company, Aiken, South Carolina, April 21, 1999.

INTERNAL DISTRIBUTION

- | | |
|---------------------|-------------------------------------|
| 1. K. K. Anderson | 21. C. H. Mattus |
| 2. D. A. Bostick | 22. C. P. McGinnis |
| 3. C. W. Chase | 23. R. R. McMahon |
| 4. J. L. Collins | 24. L. E. McNeese |
| 5. R. L. Cummins | 25. S. A. Richardson |
| 6. M. D. Griffith | 26. S. M. Robinson |
| 7. D. W. Heatherly | 27–29. P. A. Taylor |
| 8. J. D. Hewitt | 30. K. R. Thoms |
| 9. M. T. Hurst | 31. J. R. Travis |
| 10. H. L. Jennings | 32. J. F. Walker |
| 11. R. T. Jubin | 33. Central Research Library |
| 12–14. T. E. Kent | 34. ORNL Laboratory Records–RC |
| 15. D. D. Lee | 35–36. ORNL Laboratory Records–OSTI |
| 16–20. A. J. Mattus | |

EXTERNAL DISTRIBUTION

37. L. Balmer, Pacific Northwest National Laboratory, 902 Battelle Blvd., Richland, WA 99352
38. L. D. Bustard, Sandia National Laboratories, P.O. Box 5800, MS: 0728, Albuquerque, NM 87185-5800
39. J. T. Carter, Westinghouse Savannah River Company, Bldg. 704-3N, Room S151, Aiken, SC 29808
40. E. I. Cruz, U.S. Department of Energy, P.O. Box 550, MSIN: H6-60, Richland, WA 99352
41. F. Damerow, West Valley Nuclear Services, P.O. Box 191, West Valley, NY 14171
42. I. L. Drake, Jr., U.S. Department of Energy, 10282 Rock Springs Road, West Valley, NY 14171
43. Dennis Fennelly, UOP LLC, 307 Fellowship Road, Suite 207, Mt. Laurel, NJ 08054
44. S. D. Fink, Westinghouse Savannah River Company, P.O. Box 616, 773-A, Room B112, Aiken, SC 29808
45. M. W. Geeting, Westinghouse Savannah River Company, Bldg. 704-3N, Room S111, Aiken, SC 29808
46. P. W. Gibbons, Numatec Hanford Corporation, P.O. Box 999, MS: K9-91, Richland, WA 99352
47. R. L. Gilchrist, Pacific Northwest National Laboratory, P.O. Box 999, MS: K9-91, Richland, WA 99352
48. T. S. Gutmann, U.S. Department of Energy, Savannah River Operations Office, P.O. Box A, Aiken, SC 29802
49. H. D. Harmon, Tanks Focus Area at Savannah River, Bldg. 704-3N, Room N111, Aiken, SC 29808

50. R. N. Hinds, Westinghouse Savannah River Company, Bldg. 704-3N, Room S162, Aiken, SC 29808
51. E. W. Holtzscheiter, Westinghouse Savannah River Company, Savannah River Technology Center, Building 773-A, Room A-229, MS: 28, Aiken, SC 29808
52. J. O. Honeyman, CH2M Hill (CHG), P.O. Box 1500, MS: H6-62, Richland, WA 99352
53. R. A. Jacobs, Westinghouse Savannah River Company, Bldg. 704-3N, Room S311, Aiken, SC 29808
54. R. T. Jones, Westinghouse Savannah River Company, Bldg. 704-3N, Room S122, Aiken, SC 29808
55. J. Krumhansl, Sandia National Laboratories, P.O. Box 5800, MS: 0750, Albuquerque, NM 87185-0750
56. L. Li, Pacific Northwest National Laboratory, 902 Battelle Boulevard, Richland, WA 99352
57. K. A. Lockie, U.S. Department of Energy, Idaho Operations Office, 750 DOE Place, MS: 1145, Idaho Falls, ID 83402
58. J. W. McCullough, Jr., DOE at Savannah River, Bldg. 704-3N, Room S101, Aiken, SC 29808
59. J. P. Morin, Westinghouse Savannah River Company, Savannah River Technology Center, Bldg. 703-H, Room 119, Aiken, SC 29808
60. J. R. Noble-Dial, U.S. Department of Energy, Oak Ridge Operations Office, P.O. Box 2001, Oak Ridge, TN 37830-8620
61. Arlin Olson, Idaho National Engineering and Environmental Laboratory, Bldg. 637, MS-5218, Idaho Falls, ID 83415-5218
62. L. M. Papouchado, Westinghouse Savannah River Company, P.O. Box 616, 773-A, Room A263, Aiken, SC 29808
63. S. F. Piccolo, Westinghouse Savannah River Company, Bldg. 704-3N, Room S152, Aiken, SC 29808
64. J. A. Pike, Westinghouse Savannah River Company, Bldg. 704-196N, Room N401, Aiken, SC 29808
65. J. M. Reynolds, U.S. Department of Energy, Savannah River Operations Office, Bldg. 704-196N, Room S441, Aiken, SC 29808
66. Lynne Roeder-Smith, TFA Communications, Pacific Northwest National Laboratory, P.O. Box 999, MSIN K9-69, Richland, WA 99352
67. S. N. Schlahta, TFA Salt Waste Processing Program, Westinghouse Savannah River Company, Bldg. 704-3N, Room N121, Aiken, SC 29808
68. W. W. Schultz, 12704 Sandia Ridge Place NE, Albuquerque, NM 87111
69. Y. Su, Pacific Northwest National Laboratory, 902 Battelle Boulevard, Richland, WA 99352
70. P. C. Suggs, U.S. Department of Energy, Savannah River Operations Office, Bldg. 704-196N, Room S431, Aiken, SC 29808
71. W. L. Tamosaitis, Westinghouse Savannah River Company, P.O. Box 616, 773-A, Room A231, Aiken, SC 29808
72. Tanks Focus Area Headquarters Program Lead, c/o Kurt Gerdes, DOE Office of Science and Technology, 19901 Germantown Road, 1154 Cloverleaf Building, Germantown, MD 20874-1290
73. Tanks Focus Area Program Manager, c/o T. P. Pietrok, U.S. Department of Energy, Richland Operations Office, P.O. Box 550, MS: K8-50, Richland, WA 99352

- 74–81. Tanks Focus Area Technical Team, c/o B. J. Williams, Pacific Northwest National Laboratory, P.O. Box 999, MSIN K9-69, Richland, WA 99352
82. Larry Tavlarides, Syracuse University, Dept. of Chemical Engineering and Materials Science, 334 Hinds Hall, Syracuse, NY 13244-1190
83. M. T. Terry, Los Alamos National Laboratory, P.O. Box 999, MSIN K9-91, Richland, WA 99352
84. T. R. Thomas, Lockheed Martin Idaho Technologies Company, P.O. Box 1625, MSIN 3458, Idaho Falls, ID 83415-3423
85. T. A. Todd, Idaho National Engineering and Environmental Laboratory, Bldg. 637, MS-5218, Idaho Falls, ID 83415-5218
86. J. H. Valentine, Lockheed Martin Idaho Technologies Company, P.O. Box 1625, MS: 3204, Idaho Falls, ID 83415-3204
87. George Vandegrift, Argonne National Laboratory, Bldg 205, 9700 South Cass Avenue, Argonne, IL 60439
88. D. D. Walker, Westinghouse Savannah River Company, P.O. Box 616, 773-A, Room B124, Aiken, SC 29808
89. D. W. Wester, TFA System Lead, Pacific Northwest National Laboratory, 902 Battelle Boulevard, P.O. Box 999, MS: P7-25, Richland, WA 99352
90. W. R. Wilmarth, Westinghouse Savannah River Company, P.O. Box 616, 773-42A, Room 153, Aiken, SC 29808